

X-Ray Imaging of Coronary Stents

R. SCHMIEDL, M. SCHALDACH

Department of Biomedical Engineering, University of Erlangen-Nuremberg, Germany

Summary

Accurate imaging of vessels and vessel implants is an essential prerequisite for the guidance of interventional procedures and the assessment of their early and late outcome. Physicians, physicists, and technicians have long been familiar with X-ray imaging as well as developing this technique into a well-established routine method with general applicability and acceptance. However, the degree of quantitative precision required to meet the potential of current cardiovascular interventional equipment is a challenge even for present-day fluoroscopy systems, especially with such delicate structures as coronary stents. This article investigates the capability of X-ray imaging in a very general approach based on the physical foundations of the method. Factors affecting the success of the imaging process are the mechanisms that determine contrast formation and spatial resolution, but also aspects of image perception and interpretation. The survey of both the information content and the inherent limitations of X-ray imaging implies practical consequences for the qualitative imaging of coronary stents, and may even help to identify and eliminate possible systematic changes to quantitative data induced by structures below the resolution limit of the instrument.

Key Words

X-ray, angiography, stent, imaging artifacts

Introduction

During the past decades, minimally invasive techniques have been developed to an amazing degree of perfection, and have replaced open surgery as the routine treatment in many cardiological applications. Catheter-based surgery is greatly beneficial to the patient because it minimizes peripheral damage to tissue, while the miniaturized tools employed may even increase the working precision at the actual target site [1,2].

In order to take full advantage of these benefits, correspondingly precise information about location and current status of the target lesion has to be obtained by equally minimal- or non-invasive methods during all stages of the intervention. This information is vital to formulating the diagnosis, guiding the course of the intervention, and finally determining the success of the procedure. From the beginning of vascular catheterization procedures, X-ray imaging has generally been employed for this purpose [3], and still is the method of choice today. The use of X-rays allows for higher resolution and more free access to the patient than magnetic resonance imaging (MRI), and interferes

hardly or even not at all with the interventional instrumentation *in situ*, as intravascular ultrasound imaging (IVUS) devices would do. Furthermore, roentgenograms have long been well-acquainted companions to physicians and provide routine diagnostic information for nearly all parts of the body in a way equivalent — or, in fact, complementary — to visual examination.

X-ray image formation is based on physical processes that differ from conventional optics. However, this fact not only provides for the generic information available through X-ray imaging, but also leads to resolution limits of this method that differ from accustomed optical limitations. The effects of these limits are especially likely to occur when very small structures are viewed, which certainly ranks coronary stents among the most challenging objects for imaging. It is the intention of this article to describe the information encompassed in X-ray images, as well as the limitations to be expected. Based on the processes involved in image formation, consequences for the practical imaging of coronary stents will be drawn

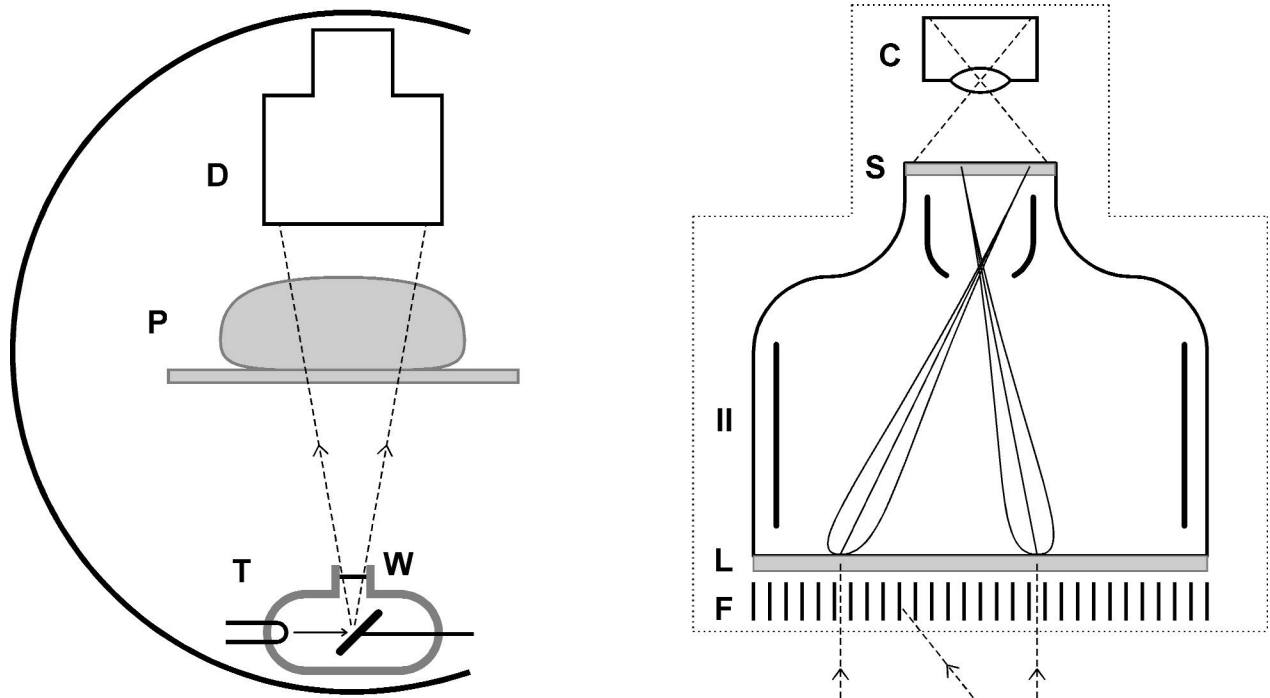


Figure 1. A fluoroscopy system (left) and details of the detector assembly (right) in a schematic view. The flow of X-rays and visible light is indicated by dashed lines, while thin full lines represent sample trajectories of electrons. See text for a description of individual components.

and discussed as examples. Although they are of great practical significance, considerations concerning radiation safety are not within the scope of this article. For a recent and thorough discussion of safety related issues covering biological effects, personnel exposure, shielding, etc., the reader is referred to Ref. [4].

Principles of the X-Ray Imaging Process

Instrumental Setup

The components of a typical fluoroscopy system are schematically depicted in Figure 1 [5]. X-rays are generated in a vacuum tube (T) by irradiating a metal anode with electrons accelerated by a voltage U . The tube is housed by a shielding that allows X-rays to exit only through a window (W). The window defines the angular width and energetic quality of the radiation by means of adjustable shutters and filter foils, respectively. The rays then traverse the table and the patient (P), where they are partially scattered or absorbed. As a consequence, the remaining rays now bear a shadow image of the illuminated volume, and project this pattern onto the detector assembly (D).

At the entrance of this assembly, a filter (F) is installed that may be conceived as an array of tiny lead pipes of less than a tenth of a millimeter in diameter each, with the pipe axes oriented towards the tube (T). This filter effectively absorbs rays that enter from lateral directions, i.e., rays that must have undergone scattering. Scatter radiation would otherwise make the image hazy and dull, as it bears a smooth intensity pattern that would no longer comply with simple projection rules. Conversely, unscattered X-rays entering from the tube direction may freely pass through the pipes, and are finally absorbed below in a thin fluorescent layer (L) that converts them into visible light. This light instantly provides the input pattern for the subsequent image intensifier tube (II). Image amplification starts with one more conversion, this time into photoelectrons, which are electrostatically accelerated and focused onto a fluorescent screen (S). There, they are reconverted into visible light of greatly increased intensity. At long last, this screen image may be viewed either directly or using a video camera (C). The latter is common practice today, allowing the physician to freely move the detector as well as to reproduce the image on

any number of screens, store it digitally, or apply electronic image enhancement or quantification.

Signal Flow in X-Ray Imaging

In order to analyze image formation, it is instructive to examine more closely the flow of signals involved in the imaging process. As is well known, the stream of X-rays that emerges from the tube consists of single radiation quanta, or photons, each carrying some fixed amount of energy. Most of these photons are absorbed within the patient and just take effect as undesired ionizing radiation. This energetic load to the patient is quantified in terms of the absorbed dose, which is defined as the amount of energy imparted by radiation per mass. Obviously, it is vital to keep the patient dose as low as reasonably achievable ("ALARA" principle [5]). Routine use of an image intensifier within the imaging chain has significantly reduced dose requirements and has eventually approached the fundamental dosage limits as determined by the noise level of the measurement: In a random stream of single entities, this noise level is governed by Poisson statistics and depends directly on the (square root of the) number of entities measured. Now, each X-ray photon that is absorbed in the fluorescent layer (L) creates on the order of 10^3 visible photons, the mean number varying according to the X-photon energy. With a conversion efficiency of about 10 %, these visible photons release some 10^2 photoelectrons into the intensifier tube, each of which in turn produces some 10^3 visible photons on the output screen (S). Obviously, the number of entities carrying information is lowest at the fluorescent layer (L), which makes the noise level at this stage determine the noise level of the final image. Current fluoroscopy systems therefore strive for the goal of constant image quality at the lowest possible patient dose by adjusting the latter in order to keep the entrance dose to the detector at a constant level.

Much instrumental development has focused on improving the conversion efficiency, durability, and linearity of the components of the imaging chain. For the purposes of this article, today's instruments may be considered approximately ideal in these respects. The intensity of the light emitted from the image intensifier screen (S) well reproduces the radiation collected by the detector. To be precise, the screen intensity is proportional to the radiation dose (rather than to the number of photons), since in the initial fluorescence conversion event each X-ray photon is "weighted" according to its energy.

Key Questions

Basically, from a very general point of view, an X-ray image consists of different grey shades forming shapes that correspond to the parts being imaged. This pattern is presented to the observing physician for the purpose of giving a correct diagnosis. Therefore, in order to analyze the process of X-ray imaging, the following issues have to be dealt with:

- What are the mechanisms that cause different grey tones (*contrast*) to occur in the image?
- Concerning shapes, what is the minimum size (*resolution*) that will still be imaged correctly?
- Of all the information displayed in the image, what kind is most suitable for recognition (*perception*) by the physician?

Fundamentals of Image Formation I: Contrast

Extinction of X-Rays

Contrast in the X-ray pattern may be caused by any local effect that attenuates the amount of radiation transmitted from the tube into the detector. In the range of X-ray energies typically employed in angiography (using voltages up to about 120 kV), the relevant effects are scattering and absorption, which both are based on the interaction between the X-ray photons and the electrons within the irradiated specimen.

Scattering events will change the direction of the photon, and may or may not be accompanied by some loss in photon energy (termed inelastic or Compton scattering vs. elastic or Rayleigh scattering, respectively). The probability of such events is mainly determined by the number of electrons available per volume and depends only slightly on photon energy.

In an absorption event, the photon energy is completely transferred to an electron which is thereby released from its bound state within an atom. Such a process is clearly limited to photon energies above a threshold given by the binding energy of the electron. With increasing photon energy, therefore, additional electrons from the more tightly bound inner shells of the atoms become available for absorption events, which gives rise to sharp "absorption edges" in the energy dependence. Apart from that, the overall probability of absorption decreases strongly with increasing photon energy, and increases with atomic number.

Extinction of radiation by either of these mechanisms entails that, per distance x traversed, a well-defined fraction of all photons is lost from the direct path.

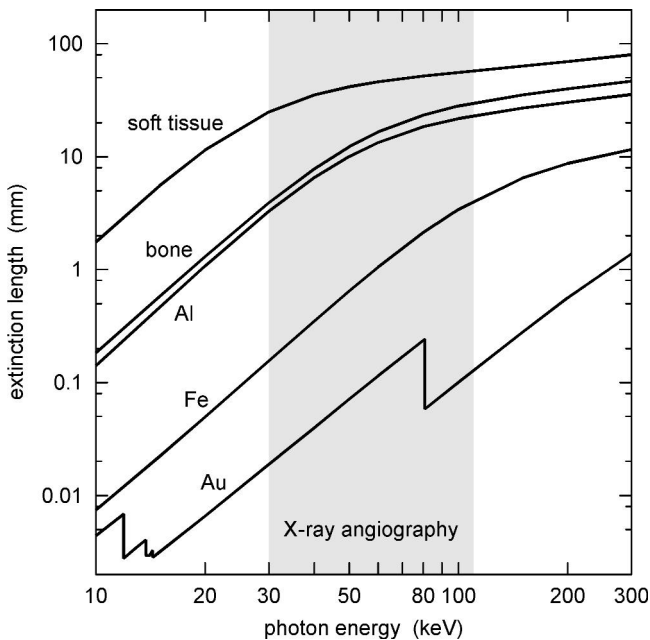


Figure 2. Energy dependence of the X-ray extinction length I for selected homogeneous materials. 1 eV (electron Volt) corresponds to the amount of energy acquired by an electron at 1 V acceleration voltage, $1 \text{ eV} = 1.6 \times 10^{-19} \text{ J}$.

For a parallel beam of photons, such a decrease in intensity I is mathematically described by Beer's Law [6],

$$(1) \quad I(x) = I_0 \cdot e^{-x/\lambda}$$

where I_0 stands for the intensity at $x = 0$, and λ is a characteristic extinction length denoting the distance required for a decrease to $1/e \approx 37\%$. The extinction length is inversely proportional to the probability of an extinction event, and thus is a function of atomic number, material density, and photon energy. Tabulated values of λ are reproduced in Figure 2 for selected organic and metallic materials. Note that the extinction length may vary between different materials by up to three orders of magnitude in the energy range most relevant to angiography. From data like those presented in Figure 2, it is straightforward to determine the attenuation of transmitted intensity, or extinction, that a given object will bring about at a given photon energy.

The X-Ray Spectrum

In order to assess the total contrast of the object, in addition to extinction data, information on the range and spectral distribution of the photon energies

involved has to be gathered, too. Generally, the X-ray spectrum as obtained from an electron-irradiated anode is a sum of two components, termed "bremsstrahlung" and "characteristic radiation".

Quanta of the former are emitted whenever electrons are decelerated in the electric field of the target nuclei. Therefore, such photons can carry any amount of energy up to the full kinetic energy of the primary electrons. The energy spectrum is continuous and decreases almost linearly to zero at the primary electron energy, as illustrated schematically by the dashed curve in Figure 3a [6]. Of all these photons, however, only those transmitted through the exit window of the tube will be available for imaging. From the extinction curves in Figure 2, it is clear that the window will remove predominantly lower-energy quanta from the initial distribution, causing the final shape of the spectrum to be a broad peak as indicated by the full line in Figure 3a.

On the other hand, characteristic radiation originates from within single target atoms that have been ionized by direct electron collision. This will provide only photons at few well-defined energies, giving rise to narrow but intense peaks that are characteristic of the emitting atom (Fig. 3a). However, in practice, this radiation is generally excluded from discussion, which may be justified by two practical arguments: On the one hand, characteristic radiation depends not only on the anode material but may even strongly vary with minor changes in acceleration voltage, especially when this voltage is only slightly above the ionization threshold (around 70 kV). The contribution of this component, therefore, is generally hard to predict. Fortunately, on the other hand, the lines of the most common anode materials W and Re are located near 60 keV, which is close to the center of the broad continuum peak under standard angiographic conditions. Thus, to a great extent, the information these lines convey is already contained in the continuum radiation image. For practical calculations, it is therefore sufficient to describe the spectrum approximately by the bremsstrahlung component only, which will allow for at least a good quantitative estimate of the contrast caused by a given object.

Calculating Image Contrast

The decisive quantity for image contrast is the intensity at the output screen. Since each photon contributes to this intensity according to its energy, the number of

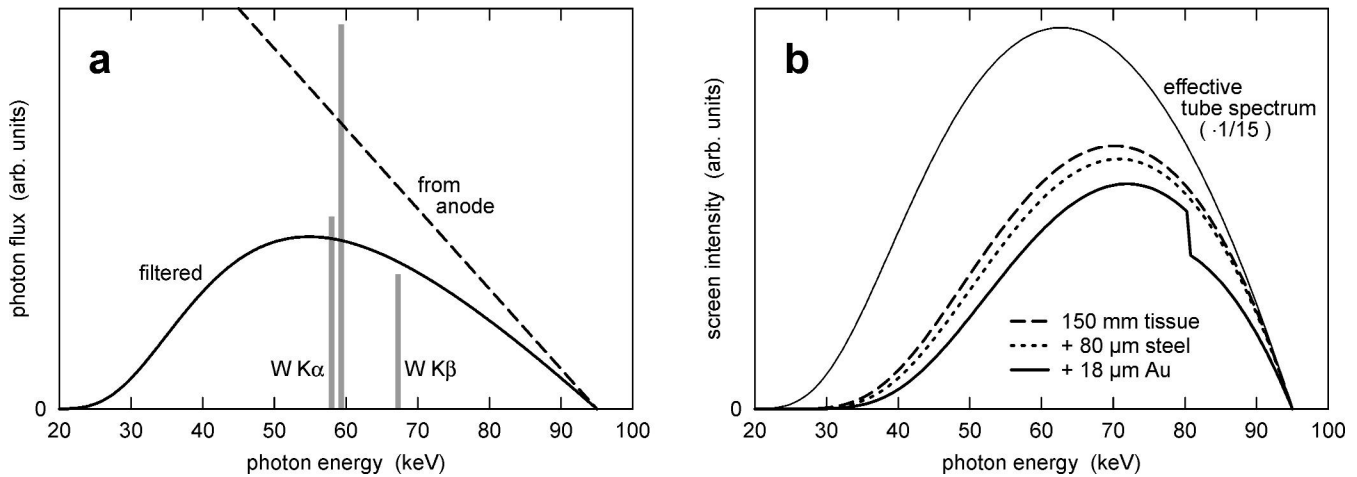


Figure 3. (a) Approximate energy distribution of X-ray photons at 95 kV electron acceleration voltage, as emitted from a W anode, and subsequently filtered by an X-ray tube exit window consisting of a 3 mm Al layer plus a 0.2 mm Cu foil. The intensity of the characteristic W radiation ($K\alpha$ and $K\beta$ lines) is not necessarily to scale. (b) Spectral contributions to the screen intensity for the imaging of a "stent strut" (iron foil) with and without a gold "marker" layer. The effective tube spectrum has been reduced by a factor of 15 for plotting.

photons, $N(E)$, has to be weighted by the photon energy E in order to render the screen effect correctly. Figure 3b displays the resulting "effective tube spectrum" which has its maximum at slightly higher energies than the photon distribution in Figure 3a. Introducing an object into the X-ray path will lead to extinction of radiation in an energy-dependent way determined by the extinction length $l(E)$ (see Figure 2) and the object thickness D , as described by Equation 1. The total screen intensity I_s may then be calculated by summing up contributions from all energies E ,

$$(2) \quad I_s \propto \int_0^{E_{max}} (E_{max} - E) \cdot e^{-D_w/l_w(E)} \cdot E \cdot e^{-D/l(E)} dE$$

where the first two factors of the integrand describe the approximate tube spectrum shown in Figure 3a, i.e., a linear decrease down to the maximum energy E_{max} combined with attenuation according to the extinction length $l_w(E)$ and thickness D_w of the exit window. The effective tube spectrum in Figure 3b is accordingly given by the first three factors of the integrand.

As an example, a typical situation for the imaging of a coronary stent is shown in Figure 3b. The object assumed consists of 150 mm soft tissue, representing a not too oblique view through a normal-weight patient [7].¹ Again, extinction removes predominantly lower-energy radiation from the spectrum, and greatly

reduces the overall intensity level (note the scaling factor applied to the effective tube spectrum for plotting). Only 4 % of the intensity without object is retained in this example, which means that 96 % of the total radiation dose is lost within the "patient". Adding a layer of iron that represents an 80 μm stent strut hardly affects the transmitted spectrum at all. Covering both sides of the iron foil with 9 μm Au, however, results in a much greater spectral change that visually indicates enhanced contrast.

In order to provide a quantitative measure of the contrast C between an "object" and the surrounding "background", the following expression is calculated:

$$(3) \quad C = \frac{I_B - I_O}{I_B + I_O} \cdot 100\%$$

where I_O and I_B denote the screen intensity within the object and background area, respectively. The use of a percentage quantity is recommended because of the eye's capability to adapt to varying illumination conditions, and by the way this renders the missing constant factor in Equation 2 irrelevant. Normalizing to the sum rather than to the larger of the two intensities yields a

¹ The air in the lungs as well as elsewhere in the imaging path can be validly neglected in these considerations due to its low and essentially constant density.

more symmetric expression and follows common practice in optics as well as in communications technology [5]. By this definition, zero contrast corresponds to equal screen intensities, while 100 % contrast means complete extinction within the object area. In the above example, the background is provided by the tissue layer alone, and contrast values of 3.4 % and 12.2 % result for the bare and the gold covered steel object, respectively. This quantifies the efficacy of a thin gold layer to produce X-ray contrast, i.e., to serve as an X-ray marker.

Contrast Limitations

As stated, current angiographic equipment does not present the intensifier output screen image directly, but records this image electronically and transfers it to a viewing screen. By electronic amplification in the course of this transfer, contrast and brightness of the resulting image may be freely adjusted, so that one might expect that in principle any non-zero contrast could be made manifest. However, the noise in the image is amplified just as much as the signal. This means that the signal intensity has a fixed percentage uncertainty that the object contrast must exceed in order to become visible. The contrast limit is therefore ultimately determined by the X-ray photon statistics that govern the noise level, and can be estimated in the following way:

The image intensifier dose commonly recommended for a single image of documentary quality is $D = 100$ nGy (nano Gray, $1 \text{ Gy} = 1 \text{ J/kg}$) when using a 17 cm entrance field [8]. As this dose is measured in terms of radiation energy per mass of *body tissue* rather than of detector material, the corresponding amount of energy is most easily calculated by assuming body tissue absorption characteristics for the detector, too, and by using infinite thickness to ensure 100 % absorption. At an irradiated area A , the absorbed energy is related to the dose via $E = D \cdot A \cdot \lambda \cdot \rho$, where λ and ρ denote extinction length and density of the hypothetical "body tissue" detector, respectively. For an average photon energy of around 60 keV, Figure 2 gives $\lambda \approx 5$ cm. This results in a total energy of $1.1 \cdot 10^{-7}$ J, which is equivalent to roughly $1.2 \cdot 10^7$ photons of 60 keV being absorbed in the detector. If the picture is formed from independent elements about 0.5 mm in size (this number will be accounted for in the next section), each element within the circular illuminated area will then receive about 130 photons, with a standard deviation of $130^{1/2} = 11.4$ photons, or 8.8 % noise level.

This consideration is of quite general validity, because the mean image intensifier dose is just the quantity that is always regulated to a pre-set value. In angiographic images, therefore, the "background" which is formed by thorax tissue of comparatively little contrast is brought to exactly this mean dose level by the image quality control loop. Although the precise numerical value of course depends on all the parameters mentioned above, practically useful parameter combinations will always end up with a similar noise level unless the dose is significantly increased. Therefore, a picture element generally should display more than about 10 % contrast in order to be classified as representing an object distinct from the background.

Fundamentals of Image Formation II: Resolution

General Considerations

Unlike visible light, X-rays cannot be focused by an optical lens. The only feasible way to transfer spatial information by means of X-rays is therefore to project a shadow image using radiation from a point source. Although such a geometric projection from a point source ideally has no inherent restrictions on resolution, real devices are made up of non-ideal components that introduce characteristic resolution limits.

When trying to quantify resolution, however, one soon realizes that there is virtually no measure of resolution that is independent of contrast. In common parlance, "low resolution" denotes a blurred image, which means that the screen intensity at any location is partially spread out over its neighborhood and averaged with contributions spread back from the surroundings. In most cases, averaging is incomplete, so that, after all, the contrast detection limit determines whether or not any remaining structure can be found in the blurred image. This limit, in turn, depends on the length scale of the measurement, as can be seen by continuing the train of thought outlined in the previous section: If the length scale of interest is given by two picture elements rather than by a single one (with all imaging conditions unchanged), the intensity level of a " 2×2 " area will be determined by $2^2 \cdot 130 = 520$ photons, with a noise level of 23 photons or only 4.4 %. In this image, therefore, a " 2×2 " object of 7 % contrast is detectable, whereas a " 1×1 " object of the same contrast is not (see Figure 4). Conversely, taking another image with just four times the dose (or equivalently, adding up four independent images of the previous dose)

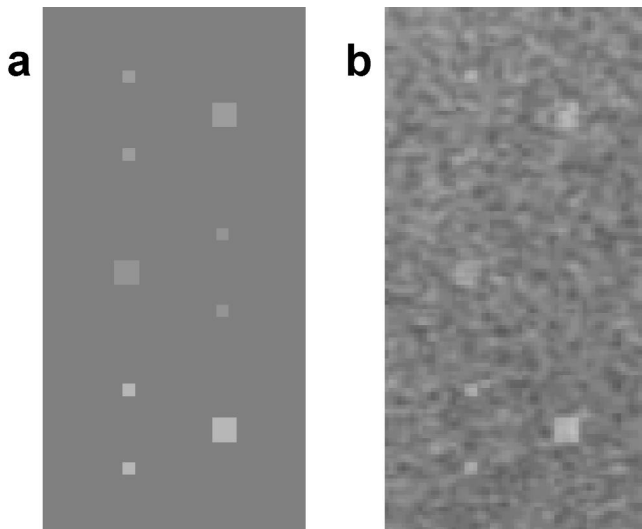


Figure 4. Contrast detection limits in a noisy image. In the test pattern (a), the contrast of the top, middle, and bottom triplet of squares is 10 %, 7 %, and 18 %, respectively. At a 9 % noise level (b), the small squares in the upper and middle set end up near and below the detection limit, respectively. However, larger objects of even the lower contrast still show up clearly against the noise, as do the small squares of higher contrast. The size of the small squares has been chosen so as to match the "independent picture element" of the noise image.

would render even the smaller object visible, although the instrument certainly has not been changed. Obviously the "resolution" that characterizes the imaging capabilities of a given fluoroscopy system is by no means a rigorous "ultimate limit", but rather denotes the "critical length scale" of the progressive contrast loss in the imaging of smaller objects.

In the context of projection, one technical remark is required to avoid possible confusion. As is clear from Figure 1, the projected pattern will always be larger than the original object, with the sizes scaling as the distances from the point source. By varying these distances, magnification factors ranging from little above 1 up to more than 2 can be achieved in practice. Correspondingly, however, resolution limits imposed by devices external to the projecting beam will yield variable apparent resolutions in the object plane. For the sake of simplicity, therefore, all resolution data given in the following account will refer to the projected image at the entrance plane of the detector rather than to the object. This will allow description of all the different effects in a consistent way, while results may readily be re-scaled to the actual object size.

Critical Length Scales for Contrast Transfer

The overall resolution of a fluoroscopy system is determined by a number of individual contributions related to the specific amount of blurring induced by each of its components. To start right within the X-ray tube [(T) in Figure 1], the non-zero size of the X-ray emitting spot will cause the shadow of a sharp object edge to form a continuous transition. The width of this transition in the projected image is given by the size of the electron-irradiated spot scaled according to the distances of detector and tube from the object edge. At a projection magnification of 1.5, for example, a 0.5 mm spot size would smear out a sharp edge across 0.25 mm in the detector plane. However, it should be noted that the specified spot size actually denotes the outer tailing of the electron distribution, while most of the radiation is emitted from well nearer to the center of the spot. Thus, actually most of the change in the image concentrates around the center of the estimated transition width, resulting in considerably (of the order of 50 %) less significant widening. During projection itself, spatial information can be degraded by photon scattering, which contributes to the image to an extent determined by the filter array [(F) in Figure 1]. With the pipes of the filter being of finite width and length, X-rays will pass through a pipe even if they enter from a direction slightly deviating from the pipe axis, i.e., after a small angle scattering event at a laterally shifted object position. However, supposing that the pipe height is 8 times the pipe diameter, the average object area from which photons will have a nonzero chance to pass, the filter will have a radius of 1/8 of the object-to-filter distance, which is a length well within the centimeter range and large compared to typical object structures. Therefore, the scattered component is sampled from so wide an area that, in effect, it merely adds up to an additional homogeneous "background" signal.²

By itself, the filter array (F) does not degrade resolution in a strict sense. However, the absorbing walls of the filter pipes inevitably introduce a regular pattern into the projected image, e.g., a 40 per mm periodicity. As this pattern is generated only just before the X-rays are absorbed, it cannot be blurred by the previous effects. Yet it certainly is an undesired addition that should not be present in the final image, and thus even creates a need for further blurring.

² Precisely this component is responsible for the increasing amount of grey veil at higher tube voltages, since scattering events prevail at higher photon energies.

In the fluorescent layer (L), each X photon releases a shower of visible photons which are no longer constrained to a specific direction. The effective photocathode area illuminated by a single shower therefore depends on the average spreading of the visible photons, for which the thickness of the absorbing layer gives an approximate (rather, upper) limit in the low 0.1 mm range.

Like the visible photons, the photoelectrons are also emitted almost isotropically into the intensifier tube (II), but the electrostatic lens formed by the electric fields within the tube forces the electrons to re-focus on the exit screen (S). However, aberrations of such a lens are inherently larger than those of an optical lens. Blurring caused by the aberrations corresponds to a width of about 0.2 - 0.3 mm in the detector entrance plane.

Finally, in the last stage of the detector assembly the image on the screen (S) is recorded by a camera and digitized into a 512×512 or 1024×1024 grid. While no perceptible image distortion is caused by the granularity of the screen phosphorus or by the camera optics, the digital recording introduces a "hard limit" on resolution, because all information possibly contained within a digital picture cell ("pixel") is replaced by the cell's average intensity. As the image intensifier allows changing of the magnification of the screen image within certain limits, the area in the detector plane that corresponds to a single cell will vary accordingly. Using a 17 cm entrance field and a 1024×1024 grid, for example, yields an effective pixel size of $17 \text{ cm} / 1024 \approx 0.17 \text{ mm}$.

With all of these components degrading resolution independently from each other, the overall critical length of contrast transfer, or overall blurring width, may be regarded as a total position uncertainty, and accordingly may be computed by quadratic addition of all the independent contributions. Taking only the lowest numbers given, one arrives at a best estimate of 0.3 mm, but standard image intensifier quality and camera pixel resolution render a value of at least 0.5 mm more realistic, especially for older fluoroscopic systems. As already stated, this length denotes a minimum size objects should have in order to be imaged without significant contrast loss. With regard to blurring, it can also be regarded as the minimum distance that must lie between two points for their intensity levels not to be mixed into each other. Still in other words, it stands for the effective size of the *smallest independent picture element*. This must not be confused with the pixel of the digital viewing monitor, which is just one contri-

bution to the former and generally corresponds to a considerably smaller distance, as shown by the values quoted above. From that, it becomes clear that objects smaller than the "resolution limit" may still show up in the final image, although their specific intensity level will have spread out into and mixed with the intensity of all the surrounding area within the reach of the estimated critical length.

Fundamentals of Image Formation III: Perception

The last step in the imaging chain — and in some respects, the most decisive one — is perception of the monitor image by the physician. This process is governed by the "technical" aspects of the human sense of sight as well as by more "non-technical" aspects of the interplay between eye and brain giving rise to object perception and interpretation [5]. Some of these aspects will be highlighted now.

"Technical" Aspects

The considerations on contrast and image noise presented above relate to single shot X-ray images. Nevertheless, images are also commonly obtained as part of a time series, e.g., within the time span of a video frame. However, it is well known that the eye is not able to perceive individual frames at such speed (which of course was chosen for exactly that reason). What is "measured" by the retina therefore corresponds rather to the *time average* of a number of frames, governed by a time constant of the order of 0.2 seconds [5]. Since the resulting retina image is thus defined by a larger dose than the single video frame, the apparent noise level will correspondingly decrease. Provided that the object does not move or change, this will improve the minimum detectable contrast, and will most probably make it possible to detect more details in a frame series than in any single frame of this series. Conversely, this effect may also be exploited the other way round in pursuit of the ALARA principle, as it allows one to use a reduced dose per frame during pulsed fluoroscopy without apparent loss in image quality. This is a common recommendation in practice [8].

In a similar way, the visual acuity may also affect the information transfer. If individual picture elements on the viewing screen cannot be resolved, they will merge into an average intensity. Consequently, the apparent resolution will degrade, although the same merging of elements will make the image look less noisy. Yet this

should not be a matter of concern in practice, since these effects may be readily controlled by proper sizing and positioning of the viewing screen.

Pattern Recognition and Interpretation

In general, the physical and neurophysiological aspects of image perception are entwined functionally just as eye and brain are anatomically. Many features only develop from the mutual interplay within the perception network, and at varying stages of abstraction. One such example, of particular significance for X-ray imaging, is the ability of the visual system to choose the length scale of interest almost at will, and even to suppress the perception of patterns on other scales once they have been identified as, e.g., "slowly varying background" or "noise". Therefore, an extended object of interest will be assigned a characteristic intensity level that is obtained by essentially an average taken across the object's area, which in turn allows the above considerations on minimum detectable contrast versus object size to be applied correspondingly.

Another example intended to illustrate the interplay of visual input and observer's knowledge in the perception process is shown in Figure 5. The black-on-white pattern presented seems quite random at first and probably even second glance. On prolonged inspection, however, the blotches eventually make sense and may be interpreted



Figure 5. Example illustrating the interplay between the information presented by the image and pattern-finding processes added by the observer during perception of the image content [5].

to depict a rider on horseback. It is most notable that once this shape has been identified, it will immediately be re-established when looking again at this image. This clearly demonstrates that a pattern that is expected or known to occur in the image can be easily perceived even if it is heavily distorted. On the other hand, unknown or unexpected shapes are liable to be regarded as random noise at a far lower level of distortion.

There is a vast number of further "non-technical" factors that affect the processes of reading, understanding, and interpreting visual information. Among them are fundamental ones like general visual ability, state of education or practical experience, or — much less easy to assess — comprehension, mental acuity, and even imagination. Other factors depend rather on the given situation, like eye adaptation time after illumination changes, fatigue of sense of sight after prolonged duty, or the presence of complications that force attention to be focused on them. Susceptibility to each of these influences may vary widely due to personal disposition, or physical condition even within one individual, and no attempt will be made here to claim enough understanding of the physiological and neurological processes involved to propose an imaging strategy that is optimized along such lines. Instead, the following discussion will focus on practical consequences for X-ray imaging that can be drawn from the general considerations presented above, with some emphasis on coronary stents.

Discussion

Imaging of Single Objects: Struts of a Coronary Stent

The general condition for X-ray visibility an object must fulfil is to provide a level of contrast within the area it is projected to that is sufficient to be detected above the noise level of the image. As a rule of thumb, about 10 % contrast will be required across the area of an independent picture element, which is commonly of the order of 0.3 - 0.5 mm in diameter with current instrumentation. An object of larger diameter may be detected at a correspondingly lower contrast, because the effective noise level decreases when short-scale variations are averaged out. However, object size is not always the length scale of interest: For example, when the borders of a large object have to be tracked down to a desired accuracy, the length scale to define the effective noise will be just the tolerance allowed. Contrast requirements will increase accordingly, as is

common experience with precision measurements. On the other hand, the characteristic contrast of objects or structures of a diameter smaller than the independent picture element will be distributed throughout an area of the size of the independent picture element, such that the contrast at a given point will be an average contrast sampled from a surrounding area of the same size. Therefore, the contrast of a small structure will only be sufficient if the 10 % limit is exceeded even after the area average has been performed.

Taking the imaging of struts of a coronary stent as an example, under idealized conditions a 12.2 % contrast has been predicted earlier for a gold/iron combination that models the sandwich structure of a strut with a "marker" layer (see Figure 3b and related text). Being typically 100 μm wide and generally much longer than the critical length of 0.5 mm (or alternatively, 0.3 mm), the strut will occupy about 20 % (33 %) of the averaging area, which decreases the maximum contrast achieved to 2.5 % (4 %). Taking into account that the side walls of the strut are also covered with gold, corresponding calculations predict that the total contrast will peak at 4 % (6.3 %) after averaging. This is clearly not enough to allow detection of a single strut under standard imaging conditions.

However, frequently another strut from the other side of the stent tube will come up next to the first strut in the projected image, thereby effectively doubling the percentage of strut area within the blurring range, and thus also doubling the resulting contrast. Similarly, contrast is enhanced if the second strut lies just within the shadow of the first one, because now extinction is nearly doubled in this area ("nearly" because the second strut receives only radiation already attenuated by the first strut). Strut-like features are therefore likely to reach the detection limit especially if the front and back sides of the stent tube appear "aligned" to each other, while "random" orientation will rather produce lower and diffuse contrast without discernible structures. The situation is illustrated in Figure 6 for a segment of a Tenax XR coronary stent (Biotronik, Germany), demonstrating that images calculated from the above considerations are found to match well to experimental data. Figure 6 also shows that, whereas the actual strut orientation is clearly a matter of chance near the tube axis, the situation is by far better defined at the sides of the stent tube. Here, several struts accumulate within each other's blurring width in more or less the same orientation, resulting in a stable contrast

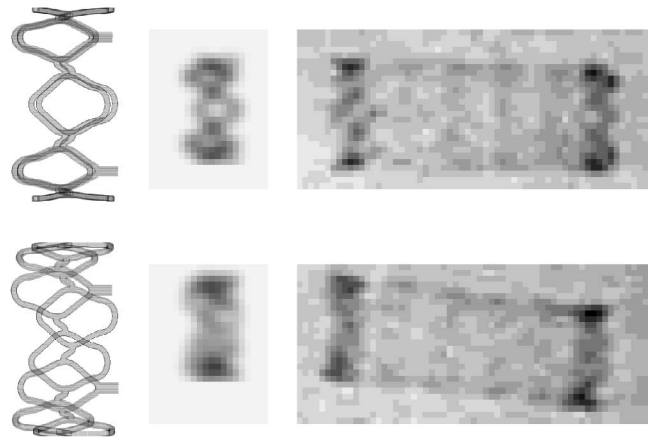


Figure 6. Effect of finite resolution on the appearance of a segment of the Tenax XR coronary stent. The upper and lower row correspond to a "near-aligned" and a "random" strut orientation, respectively. Left: Calculated ideal X-ray patterns; Middle: Same patterns but at limited resolution and scaled to the experiment; Right: Experimental images obtained with a Siemens Neurostar Plus system providing about 0.3 mm resolution.

that lies far above the detection limit. In this way, a reproducible pattern is established that is independent of a particular stent orientation and thus provides a reliable base for imaging.

Imaging of Combined Objects: Angiography of a Stented Vessel

In principle, imaging of combined objects does not introduce any fundamentally new feature apart from the obvious need to calculate the extinction by cumulating all contributions along the projection path. Again the resulting contrast may then be assessed by blurring the contrast of the ideal X-ray pattern on the scale of the critical resolution length. Trivial as this issue may seem (and essentially is), it nevertheless provides the key answer to a subtle problem that — paradoxically — arises from nothing other than sophisticated evaluation of X-ray images:

Quantitative coronary angiography (QCA) allows the diameter of a vessel to be determined with an accuracy that is better than 0.1 mm. From the above considerations, however, it is clear that information of this spatial precision is not provided by the X-ray image, at least not at normal image dose levels. Nevertheless, if some information on the object is known beforehand, the information content of the image that normally

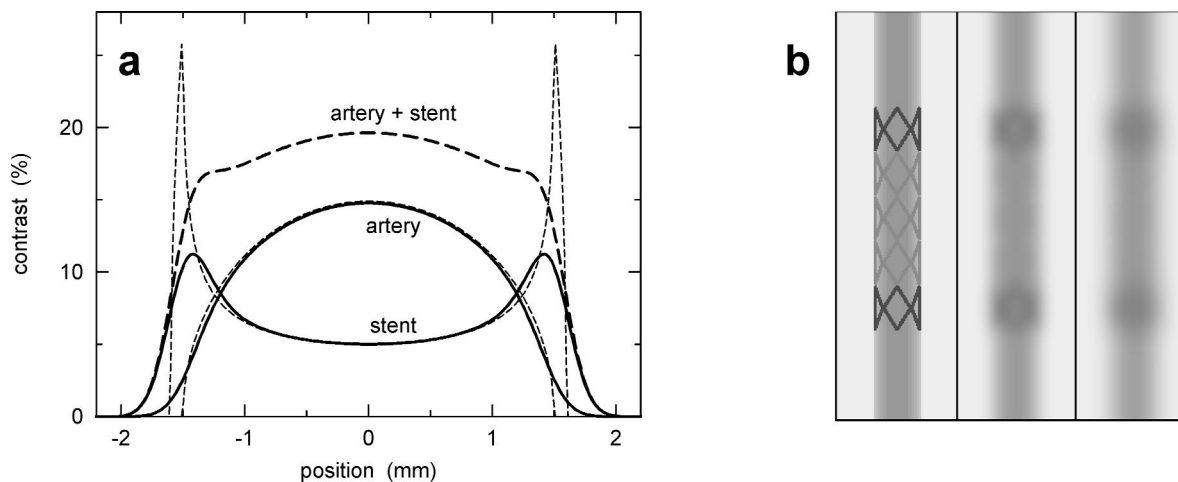


Figure 7. (a) Calculated contrast profiles for a "generalized" stent tube and a cylindrical artery, as well as the resulting profile of the stented vessel. Thin and thick lines correspond to zero and 0.3 mm blurring width, respectively. (b) Visualization of the same effect using a more realistic stent pattern resembling the X-ray characteristics of the Tenax XR stent.

would identify the object may instead be used to increase spatial precision: In the case of QCA, the object is essentially a cylindrical volume that is filled with a solution of contrast agent and is viewed perpendicular to the cylinder axis. Thus, the contrast change across the vessel diameter can be calculated theoretically for ideal imaging conditions as well as for the actual resolution of a given instrument (Figure 7a, "artery"). In the resulting profile of the contrast onset, the position of the vessel edge is exactly known from theory, which changes the task of edge detection into determining the position of the onset region within the image. However, looking for the onset pattern implies sampling data across a range equal to the predicted onset width. Due to this larger range, the corresponding noise level is substantially reduced—and thereby, positioning precision increased—as compared to sampling only across a range of the independent picture element, let alone the targeted tolerance width. In practical terms, rather than matching a calculated onset profile to patterns in the image, an "edge detection" algorithm is applied to the image that is sensitive to the desired kind of correlated changes. Results of this filtering algorithm are superimposed on the original image to present "sharpened" edges to the observing physician as well as to the software that evaluates quantitative angiographic data.

The problem mentioned arises when the QCA system is confronted with an object that has a non-cylindrical

contrast profile. While the edge of an artery is generally cylindrical to a good approximation even in an asymmetric stenosis, a stent provides an X-ray pattern with narrow regions of extreme contrast right at the edges. The "stent" curves in Figure 7 illustrate this for the case of a "generalized" stent tube, which has been calculated assuming an equivalent homogeneous material distribution across the tube surface in order to become independent of a peculiar strut configuration and orientation. Blurring the ideal patterns as in the real image most obviously redistributes the narrow stent contrast into broad peaks, while the artery edges are apparently less affected due to the smoother original profile. Therefore, the combined contrast will generally display a significantly broader pattern with a stent than without. Of course, the precise extent of broadening will depend on the actual artery and stent extinction, but calculations show that it will usually be of the order of the resolution width unless the contrast agent induces near full X-ray extinction around the artery center.³ Smaller but still significant effects are predicted even for less visible stents, e.g., with pure steel struts only. Since the QCA system does not know about the presence of the stent, this will inevitably result in local overestimation of the lumen diameter by

³ This condition is not equivalent to 100 % artery contrast on the monitor, but applies independently of the monitor's brightness and contrast settings.

about 1 - 2 times the resolution width for a stent with an X-ray opaque layer, and up to about half that value for a steel-only stent. This effect may even account for deviations from the usual correlation between QCA and IVUS that have been reported to occur within stented lesions [9], with the apparent underestimation by IVUS most probably being rather an actual overestimation of the real lumen by QCA. Moreover, QCA will not only yield a systematic error in a stented region, but may even obscure the problem's origin to the physician because filtering the image for QCA tends to suppress small contrast changes along the artery that otherwise would signify the onset of the stent (like those in the blurred patterns of Figure 7b). Thus, it is left to the physician in charge to identify this artificial broadening and to correctly interpret measured results.

Optimizing Stent Contrast

Considering that the ultimate purpose of X-ray imaging is to help provide a correct diagnosis, there are at least two diagnostic questions that lead to conflicting criteria for an optimized stent contrast: On the one hand, as an implant, the stent must allow the physician to locate it in the body, which might be vital in choosing the appropriate technique for a subsequent intervention or even for recovering a stent in one of the rare cases it is lost from the balloon. Optimizing stent visibility even under adverse instrumental resolution is possible by maximizing the extinction of the struts, i.e., by using X-ray opaque materials of high atomic number rather than steel. On the other hand, the definitive purpose of the stent is to maintain lumen patency, which is therefore the clinically important criterion of successful stent implantation. The stent thus must not impede lumen measurements in the stented region, and, accordingly, should be visible as little as possible. On the whole, "optimum" visibility is largely a matter of personal preference of the physician and cannot be achieved by a single stent once and for all.

In this respect, the Biotronik Tenax XR stent provides an interesting and unique balance between the conflicting goals described. It is a stainless steel stent made up of several circular segments where only the first and last segment bear an X-ray opaque marker layer (9 μm Au) as described above. The entire surface of the stent is covered by a hemocompatible a-SiC layer that is essentially invisible to X-rays. From the viewpoint of X-ray imaging, this design minimizes

obstruction of lumen measurements just around the stent center, which is usually located near the most critical part of the lesion. The marker thickness is such that even at the ends of the stent, only the sides of the tube present a truly significant contrast, while the artery center is still comparatively open. At the resolution capabilities of current instruments, the segment side presents an elongated shape (Figure 6) that distinguishes the marker blot from point-like noise which is prone to be filtered out either by the eye or if electronic image enhancement is applied. Moreover, the total pattern is formed by a pair of blots connected by a region of less contrast, which facilitates perception as compared to a single blot. Still, as for any other metal stent, the side effects on quantitative angiography discussed above apply, giving rise to the dumb-bell-like appearance of a stented vessel that contains contrast agent (Figure 7).

Finally, all the fundamental considerations presented above make a simple method seem feasible that should theoretically allow for improvements in stent imaging under almost any set of circumstances: It has been established that the stent contrast contained in the X-ray pattern is blurred across the range of an independent image element, whereby the contrast decreases due to mixing with surrounding intensity and eventually falls below the detection limit of the noise. Now, one approach that certainly will improve visibility is to decrease the noise; yet this requires higher dose levels which are undesired for obvious reasons. The alternative idea therefore is to increase the contrast by increasing the share of the stent pattern within the blurring range. Since the pattern originates from the stent location within the patient while the blurring is determined mainly after the detector entrance, the idea can be realized by increasing the size of the projected X-ray pattern on the detector entrance plane, in other words by retracting the detector assembly from the patient as far as compatible with the required field of view. Note that the total image dose should not be affected by this maneuver. Although this setting means using the maximum entrance field of the image intensifier, which is commonly associated with larger aberrations, these additional aberrations are well tolerated due to the larger detector entrance pattern. A net benefit of increased contrast within the stent's blurring width is expected to result, which should bring a greater fraction of the stent pattern above the detection limit and thereby improve perceptibility.

Conclusion

X-ray imaging is an invaluable tool for non-invasive diagnostic purposes. Long acquaintance of both technicians and physicians with the method has led to sophisticated and optimized equipment. However, vascular interventional techniques have only recently created the need to image increasingly fine structures in a quantitative way, with structures of only a tenth of a millimeter in size as provided by coronary stents being certainly among the most demanding objects for current imaging instrumentation. It should thus not be surprising that well-established procedures for image enhancement which have been developed and optimized for anatomical structures will in general prove detrimental to the imaging of "unexpected" additions and modifications to the vascular system; indeed these procedures were positively designed to *suppress* unwanted structures.

Therefore, the physician performing interventional procedures should be aware of the limitations of current imaging devices, and should especially keep in mind the possibility of pitfalls induced by the same image enhancement procedures that have been proven — and will continue — to be helpful in so many routine applications. In some cases, it may even be best to turn off electronic filtering entirely, which at least will show the object pattern with as little modification as possible (i.e., with only the blurring inherent to the resolution). In particular, QCA results obtained from stented vessels should be viewed with great care, since apparent broadening due to the stent contrast may easily be misinterpreted as an enlarged lumen. If this happens at the lesion site, it may result in overestimation of dilatation success; but if broadening concentrates around X-ray opaque stent ends, it may be erroneously used as the reference diameter and will lead to a corresponding underestimation of lumen gain.

Unfortunately, there is no obvious feature that would

indicate if the image is free from the discussed effects. Thus it is left to the physician's experience, acquaintance with the fluoroscopy system, and knowledge of the patient's history to decide if a given X-ray image allows one to trust one's eyes. For ultimately not the image quality, nor noise level or any other single parameter of the imaging chain will decide about the success of imaging, but only the percentage of correct diagnoses enabled.

Acknowledgement

We gratefully acknowledge the support we received from the Angiography Department at Siemens AG, Medical Engineering (Forchheim, Germany), particularly its experimental data and helpful discussions.

References

- [1] King SB. The development of interventional cardiology. *J Am Coll Cardiol.* 1998; 31(4B): 64B-88B.
- [2] Kutryk MJB, Serruys P W. *Cororary Stenting - Current Perspectives.* Martin Dunitz, London: 1999.
- [3] Forssmann W. The catheterization of the right side of the heart. *Klin Wochenschr.* 1929; 8: 2085.
- [4] Limacher MC, Douglas P, Germano G, et al. Radiation safety in the practice of cardiology. *J Am Coll Cardiol.* 1998; 31(4): 892-913.
- [5] Gebauer A, Lissner J, Schott O. *Das Röntgenfernsehen.* Georg Thieme Verlag, Stuttgart, 1974.
- [6] Gerthsen C, Kneser HO, Vogel H. *Physik.* Springer Verlag, Berlin, 1982.
- [7] DIN V 13273-7: Katheter für den medizinischen Bereich - Teil 7: Bestimmung der Röntgenstrahlschwächung von Kathetern, Anforderungen und Prüfung. 1996.
- [8] Serruys PW, Kutryk MJB. *Handbook of Coronary Stents.* Martin Dunitz, London, 2000: 307-312.
- [9] Hoffmann R, Mintz GS, Popma JJ, et al. Overestimation of acute lumen gain and late lumen loss by quantitative coronary angiography (compared with intravascular ultrasound) in stented lesions. *Am J Cardiol.* 1997; 80(10): 1277-1281.